JOURNAL OF SPACECRAFT AND ROCKETS
Vol. 34, No. 6, November–December 1997

Deployment Test Methods for a Large Deployable Mesh Reflector

Hiroaki Tsunoda,* Ken-ichi Hariu,† and Yoichi Kawakami‡
Advanced Space Communications Research Laboratory, Tokyo 101, Japan
and
Kazuo Miyoshi,§ Jun Nakagawa,** and Toshio Sugimoto**
Mitsubishi Electric Corporation, Kanagawa 247, Japan

The deployment characteristics of large structures must be evaluated by ground tests. A deployment test system is described that enables high-precision gravity canceling, in contrast to the conventional radial support test method (hanging a reflector by cables suspended from a high ceiling). A large deployable reflector composed of hexagonal pyramid-shaped modules is used in the deployment test. The reflector is deployed by a coil spring force and controlled by motors and cables for a quasistatic stable deployment motion. A magnetically suspended slider test system was developed for accurate deployment tests. We confirm that hanging at the pantograph bar is the most suitable test configuration to simulate microgravity conditions, according to one-sided model experiments and deploying force analyses using mechanism analysis software. We also establish that a vertical support method, using the developed magnetically suspended sliders, enables high-precision deployment for a large deployable mesh reflector.

Introduction

IN recent years, large deployable antennas have been developed for geostationary satellite communications using handheld terminals.[1–4] The aperture diameter of the antennas must be 10 m or more to use S-band or L-band radio frequencies. We chose an aperture diameter of 10 m to utilize the S-band frequency. S-band transmission requires that the surface accuracy be better than 2.4 mm rms, including thermal deformation, alignment error, and all other factors. Deployable truss structures and mesh surfaces are the most suitable configuration for a highly accurate reflector. Figure 1 shows the antenna system configuration. The transmit and receive antennas are separated to avoid passive intermodulation.[5]

Large deployable mesh reflectors require a high folding factor, high deploying reliability, lightweight design, and great rigidity after deployment. The lightweight design and deploying reliability are the most important factors. In the past, a two-dimensional deployable hexapod truss,[6] a modular truss,[7] and the Hexa-Link Truss[3,8] have been reported as large deployable reflectors composed of truss structures and mesh surfaces. These structures are suitable for lightweight parabolic-shaped reflectors and have demonstrated sufficient rigidity after deployment, using a scale model test and analysis.[8] However, the experimental deploying force design and evaluation methods are not clear. In particular, evaluating the deployment characteristics of large deployable structures and establishing a ground deployment test method are essential for developing large deployable reflectors.

General test methods include supporting the reflector with sliders levitated by air pressure or hanging it by cables suspended from a high ceiling.[8,9] The sliders move freely in a horizontal plane; however, they cannot follow three-dimensional motion. The cable suspension system can follow three-dimensional motion, but the resisting forces increase as the deployment progresses because the cable slant increases. Therefore, a new gravity-canceling deployment test method that can follow three-dimensional motion and reduce the resisting force in the horizontal plane must be developed to test the deployment of large reflectors. Such a deployment test method has not yet been reported.

This paper treats the Hexa-Link Truss[3,8] as the basic structure for the design of a lightweight reflector. We redesigned the large deployable reflector with an aperture diameter of 10 m, as we were concerned about the stress in the truss bars. The reflector is deployed by helical coil springs equipped in the bars, and the deploying velocity is controlled by motors and cables, for a quasistatic, stable deploying motion.

This paper will clarify ground deployment test methods for a large deployable reflector. We developed a deployment test system using magnetically suspended sliders that reduce the resistance force in the horizontal plane, as opposed to the conventional radial support test method of hanging the reflector by cables suspended from a high ceiling. An accurate evaluation of the deployment characteristics of large deployable structures can be obtained using this test system. This paper also determines which hanging method best simulates microgravity conditions in the deployment tests using magnetically suspended sliders. Finally, the deployment test methods are compared with the radial support test method of suspension from a high ceiling.

Deployable Truss Structure

Structural Design

The large deployable mesh reflector discussed in this paper is constructed using hexagonal pyramid-shaped modules. The structure of the reflector consists of a mesh surface with a deployable truss support structure. Figure 2 shows the details of the deployable truss structure. The connection points where the standoffs are affixed to the truss module are on an approximated sphere, which is the best fit for a parabolic surface. The mesh surface incorporates a gold-plated mesh and spatially determined cable network. The cable network includes a surface cable, tie cord, and back cable. Surface cables link the surface nodes, which are distributed uniformly on the parabolic surface.

The truss structure described in Ref. 8 was redesigned to realize a more lightweight reflector. The primary technical aspects of

Received March 18, 1997; presented as Paper 97-1148 at the AIAA/ASME/ASCE/AHS/ASC 38th Structures, Structural Dynamics, and Materials Conference, Kissimmee, FL, April 7–10, 1997; revision received July 22, 1997; accepted for publication Aug. 14, 1997.

*Head, On-Board Antenna Technology Section, 7F, Hayakawa-Tonakai Building, 2-12-5, Iwamoto-cho, Chiyoda-ku. Member AIAA.
†Senior Research Engineer, On-Board Antenna Technology Section, 7F, Hayakawa-Tonakai Building, 2-12-5, Iwamoto-cho, Chiyoda-ku.
‡Manager, On-Board Technology Department, 7F, Hayakawa-Tonakai Building, 2-12-5, Iwamoto-cho, Chiyoda-ku.
§Manager, Space Systems Department, Kamakura Works, 325, Kami-machiya, Kamakura.
**Senior Engineer, Space Systems Department, Kamakura Works, 325, Kami-machiya, Kamakura.

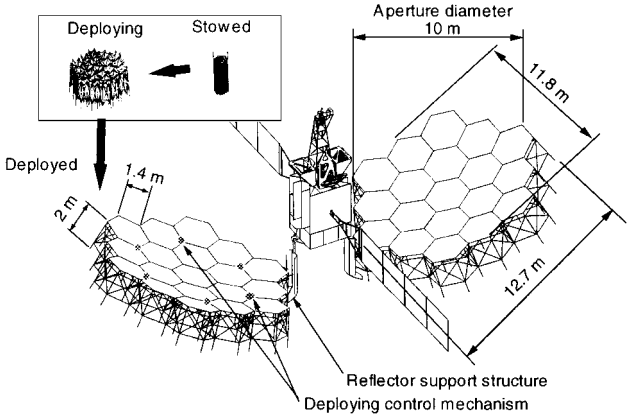

Fig. 1 Example of the antenna configuration.

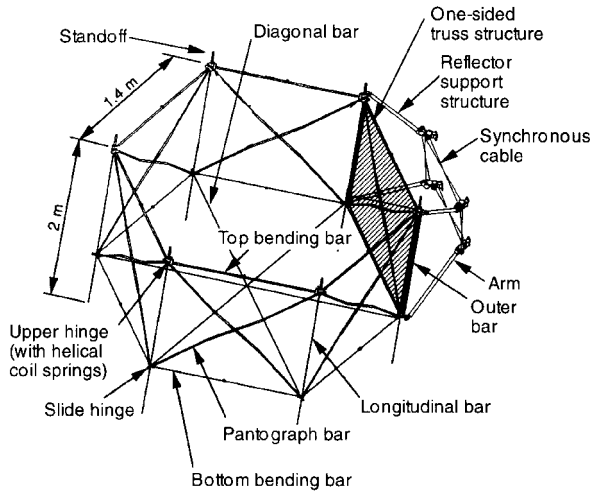

Fig. 2 Construction of the deployable truss structure.

this structure are as follows. 1) The top bending bar is forced by compression, and the bottom bending bar is forced by tension from the mesh surface reaction force. This reaction force is estimated at about 49 N. Therefore, the buckling stress of the top bending bar is over 300 N, and the tensile stress of the bottom bending bar is over 200 N. The top bending bar is made of carbon fiber reinforced plastics (CFRP) pipe with a diameter of 15 mm and a thickness of 0.5 mm. The bottom bending bar is made of CFRP rod with a diameter of 1.6 mm. 2) The diagonal bar in the truss structure supplies the truss rigidity after deployment. This bar is forced by tension in the same way as the bottom bending bar. Therefore, the same type of CFRP rod that composes the bottom bending bar was used for the diagonal bar. 3) The pantograph bars are essential for synchronous deployment. The design of the pantograph bar takes into account the stress caused by a nonsynchronous condition. Under normal deploying conditions, the pantograph bar is not forced by the spring. However, this bar is made from CFRP pipe with a drum-shaped cross section of 13 × 8 mm to resist any bending moment under anomalous deploying conditions. This bar also maintains the shape of the deployable structure. 4) The longitudinal bar restricts the rotation of the upper hinges and slide hinges. All truss structures have the joints offset; therefore, the longitudinal bar is essential to restrict the undesirable rotation of the joints. 5) The outer bar is located beside the outer longitudinal bars of the deployable structure. This bar reinforces the longitudinal bar and is forced by the bending stress. This bar is designed to be the same as the pantograph bar because the bending moment affects this bar.

The truss structure is affixed to the satellite bus using the reflector support structure. The construction of the reflector support structure is shown in Fig. 2. The one-sided truss structure of the reflector is caught by the four arms of the reflector support structure, and each joint contributes to stable deployment. The synchronous cable connects to the universal joints, which function in the synchronous deployment of the reflector support structure. This structure is deployed along with the truss structure of the reflector.

Deploying Force

The truss structure is deployed by the stored energy of the helical coil springs equipped on the top bending bar. Only the top bending bar has helical coil springs; the bottom bending bar has no springs. The springs also provide proper tensile or compressive force to all side bars after deployment, supplying a stable configuration and eliminating undesirable play in the joints. The deploying force must be maintained over the reaction force of the mesh surface during deployment. The margin around the reaction force must be considered; the design target of this margin is three times the reaction force of the mesh surface. The truss deploying force is reduced by the frictional loss of 5% caused by the truss structure joints.

To confirm the preceding deploying force estimation, we conducted an experiment and analysis of the one-sided model representing a side part of the hexagonal pyramid-shaped module. The deploying force is calculated using ADAMS® (Mechanical Dynamics, Inc.) mechanism analysis software. Figure 3a shows the analytical model of the test model. Each hinge is converted to either a spherical, universal, revolute, or translational joint. A quasistatic analysis was performed under experimental conditions. The deploying force is given by the helical coil springs and is calculated in correspondence to the deploying angle. Figure 3b shows the experiment configuration of the one-sided model. A magnetically suspended slider, described in a later section, was used for gravity cancellation. The one-sided model was suspended at the cross point of the two pantograph bars for acceptable gravity canceling characteristics. The deployment angle was measured using a potentiometer affixed to the upper hinge. (In Fig. 3b, the one-sided model hangs upside down.) The deploying force was measured by a push–pull

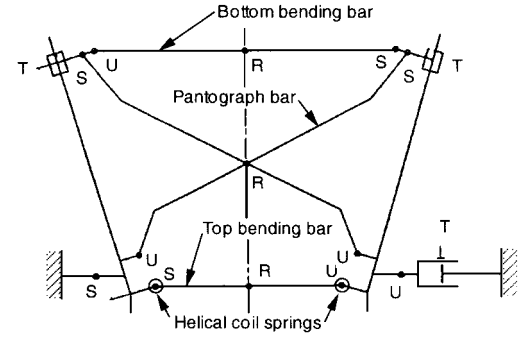

a) Analytical model

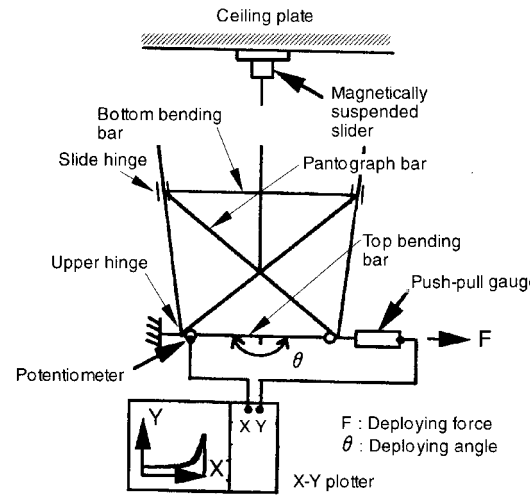

b) Experiment configuration

Fig. 3 Deploying force measurement for the one-sided model.

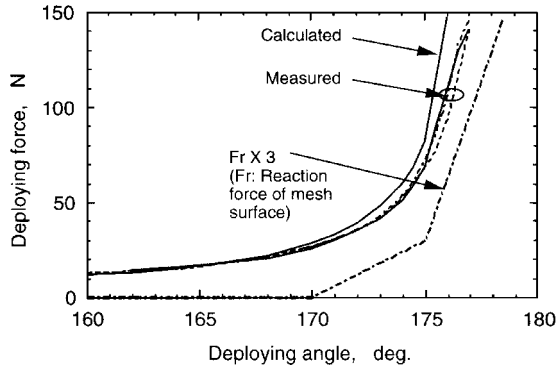

Fig. 4 Comparison of calculated and measured deploying forces.

gauge. Both measured values were plotted on an x–y plotter. The comparison between the calculated and measured deploying forces for the three sets of one-sided models is shown in Fig. 4. The deploying force was calculated with ±5% accuracy using existing spring torque. The deploying force and deploying angle were measured with ±5% and ±0.1-deg accuracy, respectively, using existing hardware and instrumentation. There was no scattering in the data from three measurements. All values measured were below the calculated values. However, it is obvious that the frictional loss was much smaller than the deploying force. The three times margin for the deploying force vs the mesh surface reaction force is confirmed.

Deploying Velocity Control

Deployment stability must be maintained to ensure reliability. However, this complicates the design in that there must be independent deploying velocity controls at each module. It is impossible for a structure to control deployment using only one motor because of the difficulty with quasistatic deployment control and the disagreement between the deploying and control directions. Therefore, in the three modules, the quasistatic deploying velocity control mechanism uses a motor and cables. This mechanism is able to control deployment directly from the upper bending bar, which has the coil springs for deploying force. The tensile stress of the control cables is 35.8 ± 1.8 N; therefore, we used stainless steel wire with a diameter of 0.6 mm for the control cables. One stepping motor with a harmonic drive gear controls the deployment of the three modules. This motor generates a torque of 1.96 (+0.34; −0.10) Nm; the gears amplify the torque to twice the value. Figure 5 shows the 19-module, full-scale reflector and 7-module partial model. The center modules of the full-scale reflector and the partial model do not have deploying velocity control mechanisms. The deploying velocity control mechanisms in the partial model are located in the same positions as on the full-scale reflector. Therefore, six motors are needed for the full-scale reflector or partial model.

Deployment Test System

Magnetically Suspended Sliders

To accomplish three-dimensional deployment motion, we developed magnetically suspended sliders. A test facility must accommodate several functions, i.e., three-degree-of-freedom active magnetic suspension control, cable tension control, cable length control, and safeguards. The deployment test configuration is given in Fig. 6. This deployment test system consisted of a magnetically suspended slider, ceiling plate, personal computer, and power supply. Commands and data transmission for the slider's movement are sent by personal computer through a digital signal processing (DSP) board. The power of the electromagnetic actuators and dc motor in the slider is supplied by a 35-V, 30-A power supply. Thirty sliders can be controlled by this system. The magnetically suspended slider moved freely in a horizontal plane under the ceiling plate. Figure 7 shows the configuration of the magnetically suspended slider. The slider diameter is 200 mm, and its height is 300 mm. Three electromagnetic actuators, consisting of permanent magnets and electromagnets, were utilized so that the slider would automatically cling to the steel ceiling plate in the event of controller trouble or power failure. Table 1 gives the target and performance of the ceiling plate.

Table 1 Specifications of ceiling plate

Item	Target	Performance
Dimensions, m	7.5 × 8	7.5 × 8
Height, m	6	6
Thickness, mm	>5	6 ± 0.6
Flatness	<1 mm /□2.4 m	<0.3 mm/□7.5 × 8 m
Joining step of each ceiling plate, mm	<0.5	0 ~ 0.5
Joining gap of each ceiling plate, mm	<0.5	0 ~ 0.5

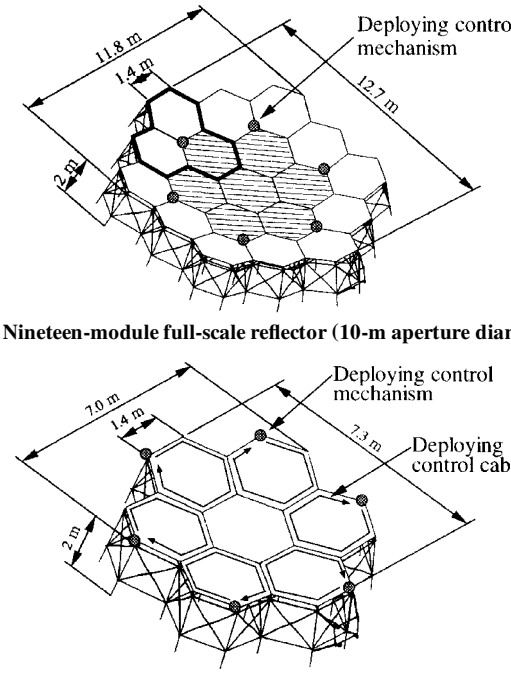

a) Nineteen-module full-scale reflector (10-m aperture diameter)

b) Seven-module partial model

Fig. 5 Development of the partial model.

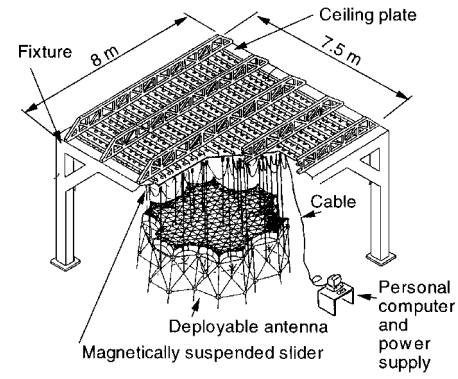

Fig. 6 Deployment test configuration using magnetically suspended slider.

The ceiling plate must be over 5 mm thick because of the attraction characteristics of the magnet. The flatness of the ceiling plates was designed and manufactured to within 1.0 mm at the 2.4-m square to suppress the drag with a horizontal motion of 0.05 N.

The maximum length of the full-scale reflector is 12.7 m, as shown in Fig. 5a. However, the partial model, as the center part of the full-scale reflector, has a maximum length of 7.3 m, as shown in Fig. 5b. The full-scale reflector is easily constructed by adding bars around the seven-module partial model. The developed deployment test facility is 7.5 × 8.0 m with a height of 6 m from the floor.

Performance of the Test System

Table 2 shows the target and the performance of the magnetically suspended slider. A maximum drag with a horizontal motion

Table 2 Specifications of magnetically suspended slider

Item	Target	Performance
Mass, kg	<4	3.5
Maximum drag with horizontal motion, N	<1	<0.25[a]
Gap (between sliders and ceiling plates), mm	<0.5	0 ~ 0.5
Maximum attractive force, N		
Control on	>90	92
Control off	>170	171
Cable tension control precision, N	<0.5	±0.25
Power consumption, W	<50	44.8
Load capacity, kg	4	2-6

[a]Slider velocity less than 0.12 m/s.

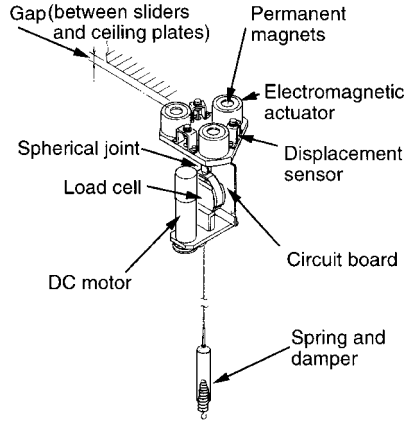

Fig. 7 Configuration of magnetically suspended slider.

of under 0.25 N, including data transmission and power supply cables, was achieved, and the control precision of the cable tension was within 0.25 N. The lightweight design of the sliders was necessary to decrease the resistance due to the slider's mass during the horizontal motion. The slider diameters were decreased to maintain the suspension wire in a vertical position in the stowed configuration. Therefore, the sliders had the 150-mm diam and 3.5-kg mass required to obtain the necessary magnetic attraction. The load capacity, i.e., the hanging mass, was 2–6 kg per slider. The maximum load capacity is assumed by adding the slider mass of 3.5 kg. A frictional coefficient of 0.01–0.02 in the horizontal motion was used when the one-dimensional deployment test system used rails. The magnetically suspended slider test system assumed a frictional coefficient of under 0.005 because of the horizontal flatness error of the ceiling plates and the resistance of the deployment control cables. A cable tension control precision of 5–10% was used in the method of suspension from one point of a high ceiling, including a frictional loss of 1–2% in the pulley. Therefore, the cable tension control precision was assumed to be under 0.5%, and the value was set under 0.5 N. Consequently, the magnetically suspended slider test method represents a three-dimensional deployment test that cannot be conducted using an air pressure suspended system.

Deployment Test Methods on the Ground

Suspension Method and Gravity Cancellation

The hanging position of the reflector during the deployment tests is the most important factor in an accurate estimation of deployment characteristics. Therefore, we compared some hanging positions by experiments using the one-sided model. In addition, the calculation was conducted under microgravity conditions. The hanging method of the one-sided model and the experiment configuration are shown in Fig. 8a. Figure 8b shows the measured and calculated deploying force of the one-sided model. The deploying force was calculated with ±5% accuracy using existing spring torque. The deploying force and deploying angle were measured with ±5% and ±0.1-deg accuracy, respectively, using existing hardware and instrumentation. The indicated values are the average of the deploying and stowing results. The deploying force is applied to the top bending bar. The gravity is canceled by suspension from a high ceiling (10 m) using constant load springs. The deploying angle and the deploying force

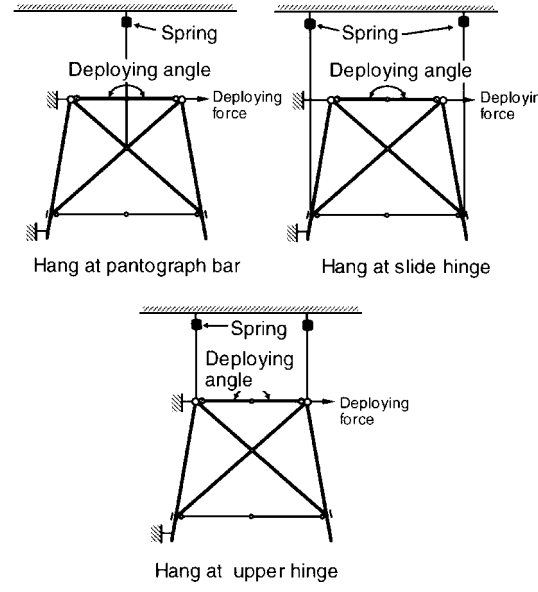

a) Experiment configuration

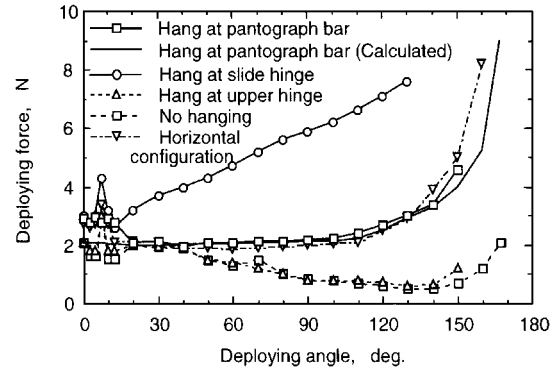

b) Deploying angle vs deploying force

Fig. 8 Comparison of hanging positions.

are measured by a potentiometer and push–pull gauge. The experiment models were hung at the slide hinges, the pantograph bar, or the upper hinge, or they were not hung. We also conducted the experiment using the horizontal configuration to obtain data from near-microgravity conditions. The analysis was conducted using ADAMS software, as described in an earlier section. The deploying force was analyzed for the hanging at the pantograph bar because this yielded results similar to the horizontal configuration. Some error factors were considered in the analysis, such as a spring torque error of 3%, a frictional coefficient of 0.3 ± 0.05 at the rotation hinges, and a frictional coefficient of 0.2 ± 0.1 at the slider hinges. Suspension at the upper hinges and no hanging suggest lower deploying force characteristics; therefore, these methods do not agree with microgravity conditions. The hanging at the slide hinges increases the deploying force during deployment. The deploying force using the pantograph bar hanging method was about equal to that of the horizontal configuration, which simulated microgravity conditions. The experimental method was also evaluated by its good agreement with the analytical values. However, both results show some difference around the peak at the beginning of deployment, possibly because the link mechanism at the upper bending bar passes a singular point.

Effects of the Magnetically Suspended Test System

The effects of the gravity-canceling methods were compared using calculations. The analytical model is a two-dimensional model that is connected by some modules in the reflector radial direction. This is not a strict analysis but is sufficient for comparing the characteristics of the suspension methods. Figure 9 shows the analytical model configurations of the traditional deployment test system and the magnetically suspended slider test system. Types

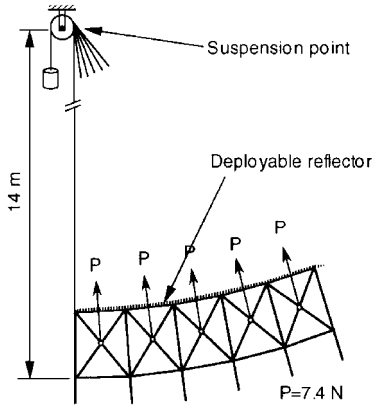

a) Radial support and pantograph hanging (type A)

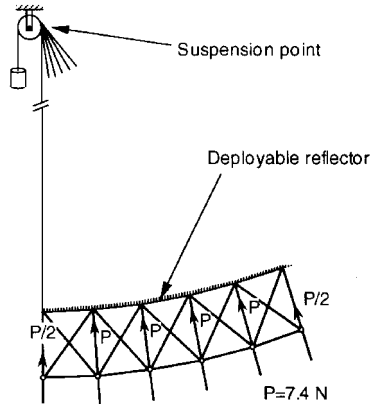

b) Radial support and slide-hinge hanging (type B)

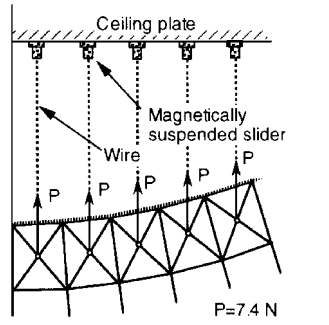

c) Vertical support and pantograph hanging (type C)

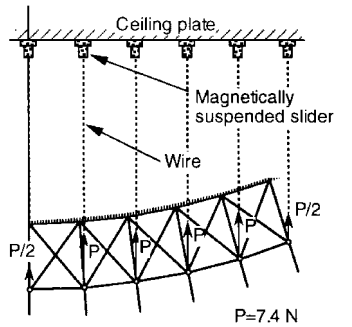

d) Vertical support and slide-hinge hanging (type D)

Fig. 9 Comparison of suspension methods.

A and B demonstrate hanging by cables suspended from a point on a high ceiling. Types C and D demonstrate the system we developed using magnetically suspended sliders. Types A and C use the pantograph hanging method, and types B and D use the slide hinges hanging method. Figure 10 gives a calculated comparison of these four suspension methods. The deploying force was calculated with ±5% accuracy using existing spring torque. It is clear that the radial support method does not simulate microgravity conditions because the deploying force is below the analytical values of

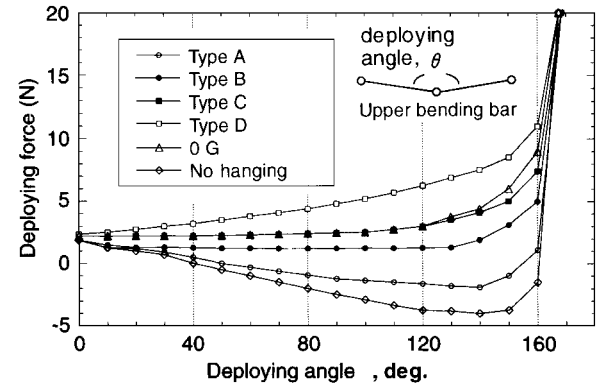

Fig. 10 Effect of gravity canceling.

microgravity conditions. In particular, the radial support and pantograph hanging method (type A) cannot deploy under microgravity conditions because the deploying force drops to under 0 N during deployment. The gravity-canceling load is decreased because of an increase in the angle between the vertical line and the suspension cable; in addition, this load forces the structure against the deployment direction. The reflector was deployed by the radial support and slide-hinge hanging method, even though microgravity conditions were not simulated. Apparently, a portion of the potential energy lost by the gravity-canceling mass helps the deploying energy. The vertical support using a magnetically suspended slider system and the pantograph hanging method (type C) efficiently simulated microgravity conditions.

Conclusions

A deployment test system using magnetically suspended sliders and test methods for an accurate deployment test for large deployable space structures, such as mesh reflectors, were proposed. This test method decreases the deploying resistance force in the horizontal plane, in contrast to the conventional radial support test method of hanging a reflector by cables suspended from a high ceiling. The magnetically suspended slider test system is therefore suitable for a deployment test of large structures. The large deployable reflector that we described in this paper was deployed by helical coil springs equipped in the bending bars; the resisting force due to the mesh surface and surface cables increased just before the deployment completion. The designed deployment force was set to be three times the mesh reaction force to achieve deployment against the mesh reaction force. In addition, a deploying velocity control mechanism using motors and cables was installed for a quasistatic deployment motion for the large deployable reflector.

A hanging method that simulates microgravity conditions using magnetically suspended sliders is proposed. The experiments and analyses revealed that hanging at the cross point of the pantograph bars is the most suitable method and agrees well with analysis under microgravity conditions. A deploying force analysis using an analytical model connecting some modules was conducted, and the results were compared with those of the conventional radial support test method of hanging a reflector by cables suspended from a high ceiling to confirm the advantages of the magnetically suspended slider system. It was demonstrated that a deployment test system using magnetically suspended sliders enables the maximum drag with a horizontal motion of less than 0.25 N and a cable tension control precision of within 0.25 N.

Acknowledgments

The authors would like to thank Yuichi Otsu for his valuable contributions to the system studies. We are also grateful to Kazuhiko Yoneyama for his helpful suggestions. The authors would like to specifically acknowledge the contributions of Takahiko Noda, Hiroyuki Naruki, and Mitsuteru Yamato for their support and suggestions.

References

[1]Taylor, S. C., and Adiwoso, A. R., "The Asia Cellular Satellite System," *Proceedings of AIAA 16th International Communications Satellite Systems*

Conference, AIAA, Reston, VA, 1996, pp. 1239–1249 (AIAA Paper 96-1134).

[2]Kai, T., and Xinhau, L., "Satellite Mobile Communications in China and APMT," *47th International Astronautical Congress*, International Astronautical Federation, IAF Paper 96-M.3.08, Beijing, PRC, 1996.

[3]Ebisui, T., Iso, A., Orikasa, T., and Okamoto, T., "Characteristics of Deployable Mesh Reflector Antenna Models for Future Mobile Communications Satellite," *Transactions of the Japan Society for Aeronautical and Space Sciences*, Vol. 39, No. 123, 1996, pp. 101–112.

[4]Tsunoda, H., Meguro, A., Miyasaka, A., and Watanabe, M., "Large Deployable Antenna Configuration for Future Communication Satellite," *47th International Astronautical Congress*, International Astronautical Federation, IAF Paper 96-I.1.02, Beijing, PRC, 1996.

[5]Ueno, K., Ohira, T., Tsunoda, H., and Ogawa, H., "Phased Array Fed Single Reflector Antenna for Communication Satellite," *Proceedings of International Symposium on Antenna and Propagation*, Inst. of Electronics, Information, and Communication Engineers, Chiba, Japan, 1996, pp. 333–336 (2C2-3).

[6]Onoda, J., Fu, D., and Minesugi, K., "Two-Dimensional Deployable Hexapod Truss," *Journal of Spacecraft and Rockets*, Vol. 33, No. 3, 1996, pp. 416–421.

[7]Watanabe, M., Meguro, A., Mitugi, J., and Tsunoda, H., "Module Composition and Deployment Method on Deployable Modular-Mesh Antenna Structures," *Acta Astronautica*, Vol. 39, No. 7, 1996, pp. 497–505; see also International Astronautical Federation, IAF Paper 95-I.6.05, Oslo, Norway, Oct. 1995.

[8]Akaishi, A., Okamoto, T., Tanizawa, K., Ebisui, T., and Ohkubo, K., "Scale Model Characteristics of Large Deployable Mash Reflector Antenna," *Proceedings of the 19th International Symposium on Space Technology and Science*, 1994, pp. 711–716 (ISTS-94-i-21).

[9]Levine-West, M. B., and Salama, M. A., "Mode Localization Experiments on a Ribbed Antenna," *AIAA Journal*, Vol. 31, No. 10, 1993, pp. 1929–1937.

H. L. McManus
Associate Editor